CrystEngComm

Hydrogen-bonded metallosupramolecular helices composed of a nona-protonated spherical $Rh^{III}_4Zn^{II}_4$ cluster with twelve carboxylate arms

Journal:	*CrystEngComm*
Manuscript ID	CE-COM-01-2020-000133.R1
Article Type:	Communication
Date Submitted by the Author:	17-Feb-2020
Complete List of Authors:	Yamashita, Ukyo; Osaka University, Department of Chemistry, Graduate School of Schience Yoshinari, Nobuto; Osaka University, Department of Chemistry, Graduate School of Schience Sodkhomkhum, Rapheepraew; Osaka University, Department of Chemistry, Graduate School of Schience Meundaeng, Natthaya; King Mongkut's Institute of Technology Ladkrabang, Department of Chemistry, Faculty of Science; Osaka University, Department of Chemistry, Graduate School of Schience Konno, Takumi; Osaka University, Department of Chemistry

COMMUNICATION

Hydrogen-bonded metallosupramolecular helices composed of a nona-protonated spherical $Rh^{III}_4Zn^{II}_4$ cluster with twelve carboxylate arms

Received 00th January 20xx,
Accepted 00th January 20xx

DOI: 10.1039/x0xx00000x

Ukyo Yamashita,[a] Nobuto Yoshinari,[a] Rapheepraew Sodkhomkhum,[a] Natthaya Meundaeng,[a,b] Takumi Konno*,[a]

Treatment of an octanuclear $Rh^{III}_4Zn^{II}_4$ cluster containing 12 free carboxylate groups, $K_6[Rh_4Zn_4O(L\text{-}cys)_{12}]$ (K_6[1], L-H_2cys = L-cysteine), with inorganic acids (HX = HBr, H_2SO_4) produced ionic crystals of $[H_9\mathbf{1}]X_3$ composed of nona-protonated $[H_9\mathbf{1}]^{3+}$ cations and X anions. The H-bonded metallosupramolecular helices in $[H_9\mathbf{1}]X_3$, which showed proton conductivity and ammonia adsorption, were controlled by inorganic anions employed.

Polycarboxylates containing two or more carboxylate groups in one molecule have been utilized not only as a raw material for organic synthesis,[1] but also as a bridging ligand for metal-organic frameworks (MOFs) or polynuclear metal complexes,[2,3] owing to their excellent Lewis basicity and chemical stability. In recent years, polycarboxylic acids, which are the conjugated acid of polycarboxylates, have attracted much attention to construct hydrogen-bonded organic frameworks (HOFs) as a next-generation porous material that possesses both permanent porosity and solubility.[4-6] For example, the hexagonal HOFs consisting of C_3-symmetric arene hexacarboxylic acids, which are soluble in halogenated solvents, have been reported to show gas-adsorption and molecular encapsulation in the solid state.[5] However, most of single-component HOFs are constructed using 2D polycarboxylic acids, and the self-organization of 3D polycarboxylic acids into HOFs have rarely been investigated.[6] This is because of the synthetic difficulty in the introduction of many carboxy groups into 3D hydrocarbon frameworks. As an alternative to organic polycarboxylates, metal clusters or nanoparticles bearing non-coordinating carboxylate groups have recently been developed.[7,8] In general, such cluster polycarboxylates contain 10-200 carboxylate groups in one molecule,[7] and most of them are difficult to be crystallized in a single species due to their polydispersity. Therefore, the crystallization of atomically precise cluster polycarboxylates into a hydrogen-bonded framework, in particular, with the control of their spatial arrangement by changing external factors, is still a great challenge.

We have been interested in the stepwise synthesis of robust thiolato-bridged metal clusters, which possess free carboxylate groups available for their further aggregation with metal ions, using natural thiol-containing amino acids, such as L-cysteine (L-H_2cys) and D-penicillamine.[9-13] A representative example is a spherical octanuclear $Rh^{III}_4Zn^{II}_4$ cluster with a hexavalent negative charge, $[Rh_4Zn_4O(L\text{-}cys)_{12}]^{6-}$ ($[\mathbf{1}]^{6-}$), which is synthesized from the L-cys rhodium(III) complex (*fac*-$[Rh(L\text{-}cys)_3]^{3-}$) and Zn^{2+} in water.[12,13] Recently, we have reported that $[\mathbf{1}]^{6-}$ crystallizes with K^+ in water to produce ionic crystals of $K_6[\mathbf{1}]$, which shows a superionic conduction in the solid state due to the high mobility of hydrated K^+ ions.[13] In $K_6[\mathbf{1}]$, the $[\mathbf{1}]^{6-}$ anions are hydrogen-bonded to each other to form a *lcy* framework because of the presence of 12 free carboxylate and 12 coordinated amino groups on the surface of the $Rh^{III}_4Zn^{II}_4$ cluster. On the other hand, our attempts to crystallize the neutral hexa-protonated $[H_6\mathbf{1}]$ were unsuccessful; the addition of 6 equiv of inorganic acids to an aqueous solution of $K_6[\mathbf{1}]$ caused the immediate precipitation of $[H_6\mathbf{1}]$ as a fine powder.[13a] However, we noticed that the addition of an excess amount of acids gives a clear yellow solution, from which a crystalline product is obtained. In this paper, we report the structural characterization of the crystalline products, $[H_9\mathbf{1}]Br_3$ (**2**) and $[H_9\mathbf{1}](HSO_4)_3$ (**3**), which were obtained by using HBr and H_2SO_4 as inorganic acids, respectively. We found that **2** and **3** commonly form hydrogen-bonded helix frameworks composed of the $[H_9\mathbf{1}]^{3+}$ cluster cations, in which nine of twelve carboxylate groups in $[\mathbf{1}]^{6-}$ are protonated. Notably, the hydrogen-bonded helices in **2** and **3** are markedly different from each other dependent on the inorganic anions incorporated. To our knowledge, such a cluster-based polycarboxylate system that shows the anion-controlled formation of hydrogen-bonded helices is unprecedented. The proton conductivity and ammonia adsorption of **2** and **3** in the solid state are also reported.

Treatment of $K_6[\mathbf{1}]$ with excess HBr in water gave a clear yellow solution (pH 1.5), from which yellow needle crystals of **2** were isolated in a moderate yield.† The diffuse reflection and

[a] *Department of Chemistry, Graduate School of Science, Osaka University, Toyonaka, Osaka 560-0043 (Japan).*
E-mail: konno@chem.sci.osaka-u.ac.jp; Tel: +81-6-6850-5765
[b] *Department of Chemistry, Faculty of Science, King Mongkut's Institute of Technology Ladkrabang, Bangkok, 10520 (Thailand).*

† Electronic Supplementary Information (ESI) available: Experimental, diffuse reflection, circular dichroism (CD), and thermogravimetric data, as well as crystal structures. CCDC 1974317-1974318. See DOI: 10.1039/x0xx00000x.

CD spectra of **2** in the solid state were essentially the same as those of K_6[**1**] (Figs. S1 and S2).† This implies that the S-bridged $Rh^{III}_4Zn^{II}_4$ cluster structure in [**1**]$^{6-}$ is retained after its treatment with excess HBr in water. In the IR spectrum, **2** gave two intense C=O stretching bands corresponding to protonated COOH and deprotonated COO^- groups at 1724 cm^{-1} and 1594 cm^{-1}, respectively (Fig. 1).[14] This is indicative of the partial protonation on the carboxylate groups of [**1**]$^{6-}$ in **2**. The elemental analysis data of **2** were in agreement with a formula for the nona-protonated cluster, [H_9**1**]Br_3, rather than other protonated species, such as [H_8**1**]Br_2 and [H_{10}**1**]Br_4.†

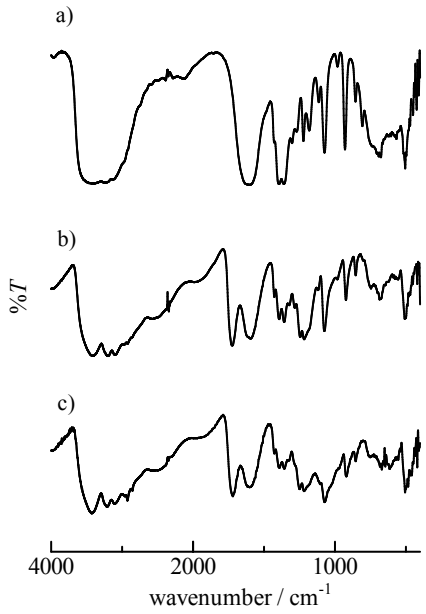

Fig. 1. IR spectra of a) K_6[**1**], b) **2**, and c) **3**.

The structure of **2**, which crystallized in the hexagonal space group of $P6_522$, was established by single-crystal X-ray crystallography.‡ In the asymmetric unit, **2** contains 0.5 cluster cation of [H_9**1**]$^{3+}$ and 1.5 Br^- anions, besides water molecules of crystallization. As expected, the overall structure of [H_9**1**]$^{3+}$ is essentially the same as that of [**1**]$^{6-}$ in K_6[**1**], although nine of twelve carboxylate groups of [**1**]$^{6-}$ are protonated (Fig. 2a).[12c] In the crystal packing, the cluster cations are connected to each other through intermolecular NH_2···OOC hydrogen bonds (av. N···O = 2.73 Å) along the crystallographic 6_5 screw axis, forming a 6-hold tubular helix with a left-handedness (*M*-helix) induced by the L-cys chirality (Figs. 2b,c). Such a chiral induction has been observed in infinite coordination systems.[15] The diameter of the helix is ca. 45 Å, and a 1D channel with a diameter of ca. 13 Å exists in the helix. Each 6-hold helix is further connected to 6 adjacent helices through NH_2···OOC hydrogen bonds (av. N…O = 2.73 Å), completing a 3D hydrogen bonding framework with a porosity of 46% (Fig. 2d,e). In addition to the N-H…O hydrogen bonds, NH_2···Br hydrogen bonds exist in **2** (av. N···Br = 3.26 Å), which appears to support the porous 3D framework (Fig. S3).† The powder X-ray diffraction (PXRD) pattern of the bulk sample of **2** matches well with the pattern simulated from the single-crystal X-ray data (Fig. 3), indicative of the homogeneity of the bulk crystals of **2**.

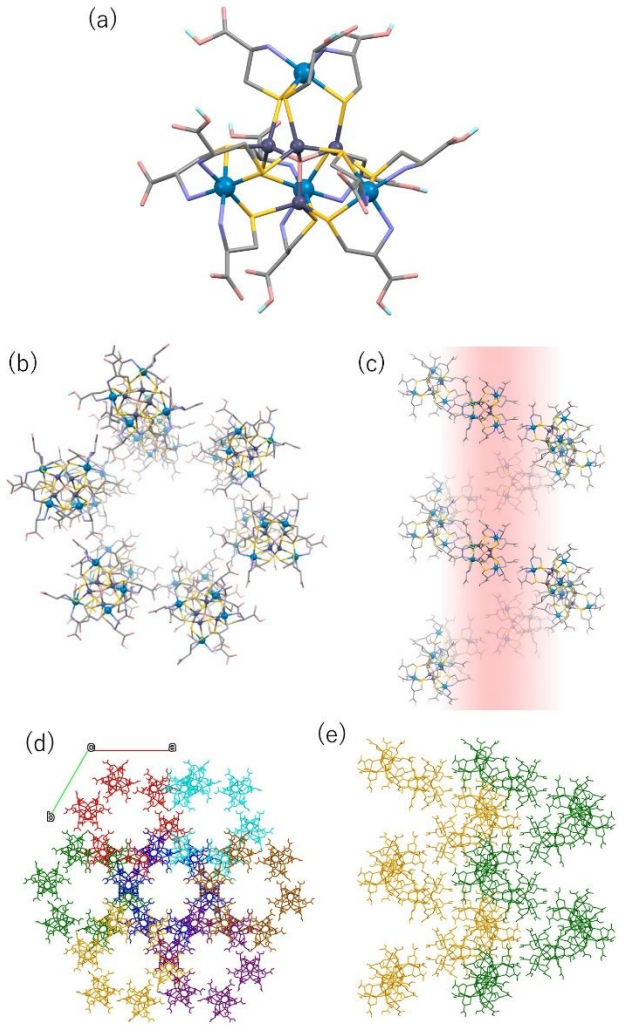

Fig. 2. Crystal structures of **2**. (a) Perspective views of the molecular structure, (b) top and (c) side views of the left-handed 6-hold helix, (d) packing structure, and (e) two neighbouring helices bridged by hydrogen bonds. H atoms except for COOH groups are omitted for clarity. Colour code: Rh, blue-green; Zn, dark grey; S, yellow; O, pink; N, blue; C, grey; H, light blue. Each helix is illustrated using different colours in (d) and (e).

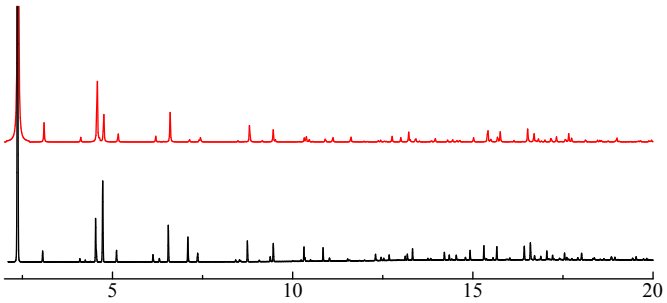

Fig. 3. The observed (black) and simulated (red) powder X-ray diffraction patterns for **2**.

A similar reaction using H_2SO_4 instead of HBr gave yellow block crystals (**3**).† The retention of the $Rh^{III}_4Zn^{II}_4$ octanuclear structure of $[\mathbf{1}]^{6-}$ was confirmed by the reflection and CD spectra of **3** in the solid state (Figs. S1 and S2).† The elemental analytical data of **3** agreed well with a formula for the nona-protonated cluster ($[H_9\mathbf{1}](HSO_4)_3$), as in the case of **2**.† The formation of $[H_{12}\mathbf{1}](SO_4)_3$, instead of $[H_9\mathbf{1}](HSO_4)_3$, is excluded because the IR spectrum of **3** exhibits two C=O stretching bands corresponding to COOH (1725 cm^{-1}) and COO^- (1621 cm^{-1}), the intensity ratio of which is similar to that for **2** (Fig. 1).[14]

The structure of **3**, which crystallized in the tetragonal space group of $P4_32_12$, was also determined by single-crystal X-ray analysis.‡ In the asymmetric unit, **3** contains a cluster cation of $[H_9\mathbf{1}]^{3+}$ (Fig. 4a) and three HSO_4^- anions, besides water molecules of crystallization. In **3**, the cluster cations are

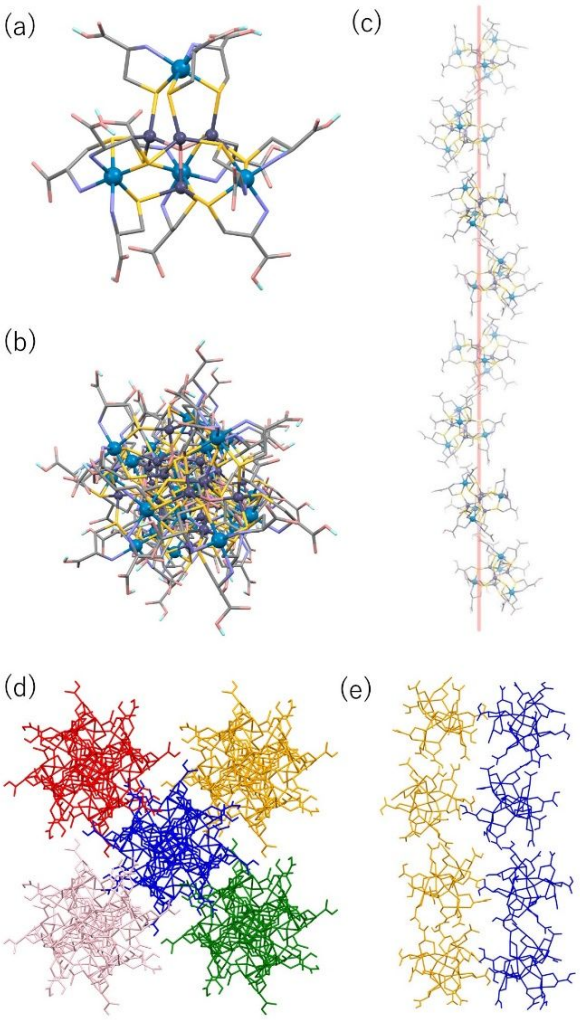

Fig. 4. Crystal structures of **3**. (a) Perspective views of the molecular structure, (b) top and (c) side views of the left-handed 4-hold helix, and (d) packing structure, and (e) two neighbouring helices bridged by hydrogen bonds. H atoms except for COOH groups are omitted for clarity. Colour code: Rh, blue-green; Zn, dark grey; S, yellow; O, pink; N, blue; C, grey; H, light blue. Each helix is illustrated using different colours in (d) and (e).

connected to each other through $NH_2\cdots OOC$ hydrogen bonds (N···O = 2.891(10) Å) along a 4_3 screw axis, forming a 4-hold helix structure with a left-handedness (*M*-helix) (Figs. 4b,c). The helix chain in **3** is moderately waved to form a non-tubular structure with a diameter of ca. 19 Å. Each helix chain is further connected with four adjacent chains through $NH_2\cdots OOC$ (av. N···O = 2.98 Å) hydrogen bonds, completing a 3D supramolecular structure with a porosity of 17% (Fig. 4d,e). In **3**, there exist additional $NH_2\cdots OSO_3$ (av. N···O = 2.93 Å) and $COOH\cdots OSO_3$ (av. O···O = 2.69 Å) hydrogen bonds between $[H_9\mathbf{1}]^{3+}$ cations and HSO_4^- anions, supporting the helical chain structure (Fig. S4).† Again, the homogeneity of the bulk sample of **3** was confirmed by the powder X-ray diffraction (PXRD) pattern that matches well with the simulated pattern (Fig. 5). Here it should be noted that the supramolecular helix structures in **2** and **3** are markedly different from each other, despite the same protonation level of the $Rh^{III}_4Zn^{II}_4$ cluster in **2** and **3**. In **2**, the Br^- ions incorporated are only participated in the formation of NH···Br hydrogen bonds, whereas the HSO_4^- ions in **3** forms both $NH\cdots OSO_3$ and $COOH\cdots OSO_3$ hydrogen bonds. It is likely that the involvement of the protonated COOH groups of $[H_9\mathbf{1}]^{3+}$ to the interaction with counter anions is responsible for the construction of the dense helix structure in **3**.

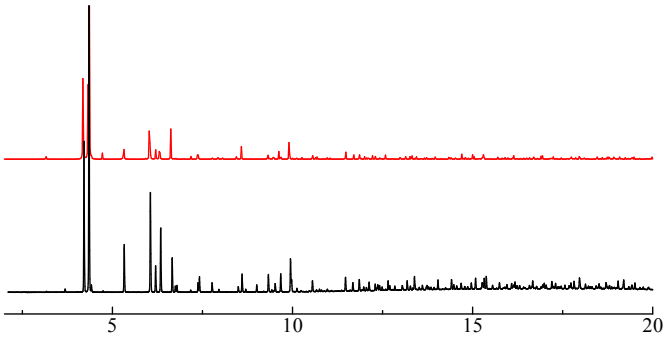

Fig. 5. The observed (black) and simulated (red) powder X-ray diffraction patterns for **3**.

To check whether supramolecular frameworks containing protonated metal clusters exhibit proton conduction in the solid state, bulk conductivities of **2** and **3** were evaluated via quasi-four probes alternate-current (ac) impedance measurements under the controlled temperature (290 K) and humidity (90 %).[16] The conductivities of **2** and **3** were $\sigma = 1.4 \times 10^{-6}$ S/cm and 4.6×10^{-6} S/cm, respectively, having the same order of conductivities. Notably, these values are more than 10^3 times higher than that of the neutral, hexa-protonated $[H_6\mathbf{1}]$ ($\sigma = 1.3 \times 10^{-9}$ S/cm). It is reasonable to assume that the positively charged $[H_9\mathbf{1}]^{3+}$ cluster can release H^+ ions from the COOH groups more easily than the neutral $[H_6\mathbf{1}]$, leading to the appreciable proton conductivities for **2** and **3**.

Prompted by our recent finding of ammonia adsorption in acidic metallosupramolecular ionic crystals,[17] ammonia-gas adsorption capacities were also investigated for **2** and **3** at 298

K (Fig. 6).[18] The ammonia adsorption isotherm for **2** displays a rapid adsorption of 3.8 mmol/g at 0.07 bar, followed by a gradual increase to 7.7 mmol/g at 0.93 bar. The initial and the total uptakes correspond to the adsorptions of 9 and 18 ammonia molecules per formula. It is assumed that the chemical adsorption of ammonia occurs around the $[H_9\mathbf{1}]^{3+}$ cations in the early stage so as to neutralize 9 COOH groups of each $[H_9\mathbf{1}]^{3+}$ cation, followed by the physical adsorption of ammonia molecules in the void spaces of the supramolecular framework in **2**. A similar ammonia adsorption behaviour was observed for **3**; a rapid adsorption of 4.0 mmol/g occurs at 0.07 bar, followed by a gradual increase to 8.1 mmol/g at 0.93 bar. Note that the ammonia adsorption capacities of **2** and **3** are larger than the record value of a HOF system (6.67 mmol/g, for KUF-1a),[19] although they are smaller than the highest capacity found in a MOF system (19.79 mmol/g for Cu_2Cl_2BBTA).[20] Since K_6[**1**] showed only a small ammonia adsorption (1.3 mmol/g), protonation on the cluster polycarboxylates is crucial for the ammonia adsorption in the present system.

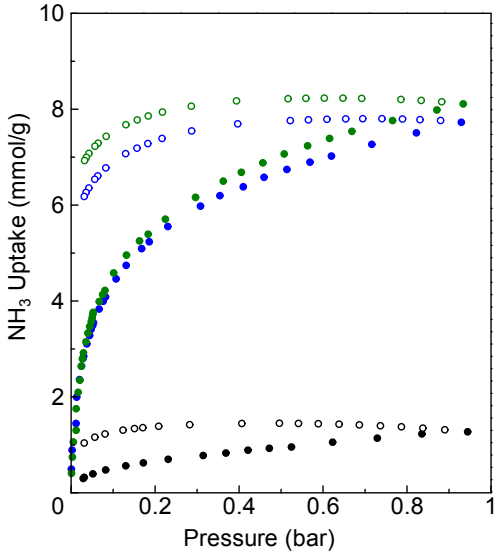

Fig. 6. NH_3 adsorption (filled circle) and desorption (open circle) isotherms of K_6[**1**] (black), **2** (blue), and **3** (green) at 298 K.

Conclusions

In summary, we showed that nine of twelve free carboxylate groups in the $Rh^{III}_4Zn^{II}_4$ cluster ($[\mathbf{1}]^{6-}$) are protonated on treatment with excess inorganic acids, HBr and H_2SO_4, affording ionic crystals of $[H_9\mathbf{1}]Br_3$ (**2**) and $[H_9\mathbf{1}](HSO_4)_3$ (**3**), respectively, that possess the functionalities of proton conduction and ammonia adsorption in the solid state. Of note is the construction of hydrogen-bonded supramolecular helices in **2** and **3**, the structures of which are quite different from each other (6-hold tubular helix for **2** vs. 4-hold dense helix for **3**). This is ascribed to the difference in the hydrogen-bonding motifs between Br^- and HSO_4^- toward $[H_9\mathbf{1}]^{3+}$. The present study that showed the construction of structurally precise hydrogen-bonding helices from $[\mathbf{1}]^{6-}$ and inorganic acids and their control by acids employed should provide insight into the controlled creation of hydrogen-bonded frameworks based on cluster polycarboxylates.

This work was supported in part by CREST, JST (Grant No. JPMJCR13L3) and by JSPS KAKENHI (Grant Nos. 18H05344, 19K05496). The synchrotron radiation experiments were performed at BL02B1 and BL02B2 of SPring-8 with the approval of JASRI (Proposal Nos. 2017B1046, 2018A1441, 2018A1476, 2018B1304).

Conflicts of interest

There are no conflicts to declare.

Notes and references

‡ *Crystallographic data for* $[H_9Rh_4Zn_4O(\text{L-cys})_{12}]Br_3\cdot 29H_2O$ (**2**): $C_{36}H_{69}Br_3N_{12}O_{54}Rh_4S_{12}Zn_4$, M = 2831.60, hexagonal, space group $P6_522$, a = 27.8380(16) Å, c = 28.8132(8), V = 19337(2) Å^3, Z = 6, T = 100(2) K, 315765 reflections collected, 14807 independent reflections, 9805 observed reflections ($I > 2\sigma(I)$), R_1 ($I > 2\sigma(I)$) = 0.043, wR_2 (all data) = 0.101, Flack parameter 0.035(5).
Crystallographic data for $[H_9Rh_4Zn_4O(\text{L-cys})_{12}](HSO_4)_3\cdot 19.5H_2O$ (**3**): $C_{36}H_{72}N_{12}O_{56.5}Rh_4S_{15}Zn_4$, M = 2731.07, tetragonal, space group $P4_32_12$, a = 19.365(3) Å, c = 52.561(4) Å, V = 19711(6) Å^3, Z = 8, T = 100(2) K, 288710 reflections collected, 21951 independent reflections, 21407 observed reflections ($I > 2\sigma(I)$), R_1 ($I > 2\sigma(I)$) = 0.0386, wR_2 (all data) = 0.1099, Flack parameter 0.0655(19).

1 A. E. Felber, M. H. Dufresne, J. C. Leroux, *Adv. Drug Deliv. Rev.* 2012, **64**, 979-992.
2 (*a*) D. Farrusseng (ed.), *Metal-organic frameworks: applications from catalysis to gas storage,* John Wiley & Sons, 2011; (*b*) H.-C. Zhou, J. R. Long, O. M. Yaghi, *Chem. Rev.* 2012, **112**, 673-674.
3 (*a*) S. Pasquale, S. Sattin, E. C. Escudero-Adán, M. Martínez-Belmonte, J. de Mendoza, *Nature Commun.* 2012, **3**, 785; (*b*) N. Ahmad, A. H. Chughtai, H. A. Younus, F. Verpoort, *Coord. Chem. Rev.* 2014, **280**, 1-27.
4 (*a*) Y. He, S. Xiang, B. Chen, *J. Am. Chem. Soc.* 2011, **133**, 14570-14573; (*b*) A. Karmakar, R. Illathvalappil, B. Anothumakkool, A. Sen, P. Samanta, A. V. Desai, S. Kurungot, S. K. Ghosh, *Angew. Chem. Int. Ed.* 2016, **55**, 10667-10671; (*c*) R.-B. Lin, Y. He, P. Li, H. Wang, W. Zhou, B. Chen, *Chem. Soc. Rev.* 2019, **48**, 1362-1389.
5 (*a*) I. Hisaki, S. Nakagawa, N. Tohnai, M. Miyata, *Angew. Chem. Int. Ed.* 2015, **54**, 3008-3012; (*b*) I. Hisaki, H. Toda, H. Sato, N. Tohnai, H. Sakurai, *Angew. Chem. Int. Ed.* 2017, **56**, 15294-15298; (*c*) I. Hisaki, S. Nakagawa, H. Sato, N. Tohnai, *Chem. Commun.* 2016, **52**, 9781-9784.
6 R. J. Butcher, A. Bashir-Hashemi, R. D. Gilardi, *J. Chem. Crystallogra.* 1997, **27**, 99-107.
7 P. D. Jadzinsky, G. Calero, C. J. Ackerson, D. A. Bushnell, R. D. Kornberg, *Science* 2007, **318**, 430-433.
8 (*a*) S. Wang, H. Yao, S. Sato, K. Kimura, *J. Am. Chem. Soc.* 2004, **126**, 7438-7439; (*b*) B. E. Conn, A. Desireddy, A. Atnagulov, S. Wickramasinghe, B. Bhattarai, B. Yoon, R. N. Barnett, Y. Abdollahian, Y. W. Kim, W. P. Griffith, S. R. J. Oliver, U. Landman, T. P. Bigioni, *J. Phys. Chem. C* 2015, **119**, 11238-11249; (*c*) T. Lahtinen, E. Hulkko, K. Sokołowska, T.-R. Tero, V. Saarnio, J. Lindgren, M. Pettersson, H. Häkkinen, L. Lehtovaara, *Nanoscale* 2016, **8**, 18665-18674.
9 (a) A. Igashira-Kamiyama, T. Konno, *Dalton Trans.* 2011, **40**,

7249-7263; (b) N. Yoshinari, T. Konno, *Bull*. *Chem*. *Soc*. *Jpn*. 2018, **91**, 790-812.
10 (*a*) T. Aridomi, K. Takamura, A. Igashira-Kamiyama, T. Konno, *Chem*. *Lett*. 2008, **37**, 170-171; (*b*) H. Q. Yuan, A. Igashira-Kamiyama, T. Konno, *Chem*. *Lett*. 2010, **39**, 1212-1214.
11 (*a*) T. Konno, N. Yoshinari, M. Taguchi, A. Igashira-Kamiyama, *Chem*. *Lett*. 2009, **38**, 526-527; (b) N. Yoshinari, T. Konno, *Dalton Trans*. 2011, **40**, 12191-2200; (c) S. Surinwong, N. Yoshinari, T. Kojima, T. Konno, *Chem*. *Commun*. 2016, **52**, 12893-12896; (d) N. Kuwamura, Y. Kurioka, T. Konno, *Chem*. *Commun*. 2017, **53**, 846-849; (e) N. Oya, M. Yamada, S. Surinwong, N. Kuwamura, T. Konno, *Dalton Trans*. 2018, **47**, 2497-2500; (f) H. Ohwaki, N. Yoshinari, T. Konno, *Chem*. *Commun*. 2019, **55**, 3402-3405.
12 (*a*) T. Konno, K. Okamoto, J. Hidaka, *Inorg*. *Chem*. 1994, **33**, 538-544; (*b*) U. Yamashita, P. Lee, N. Kuwamura, N. Yoshinari, T. Konno, *Bull*. *Chem*. *Soc*. *Jpn*. 2013, **86**, 1450-1452; (*c*) N. Yoshinari, U. Yamashita, T. Konno, *CrystEngComm* 2013, **15**, 10016-10019.
13 (*a*) N. Yoshinari, S. Yamashita, Y. Fukuda, Y. Nakazawa, T. Konno, *Chem*. *Sci*. 2019, **10**, 587-593; (*b*) "Coordination Molecular Technology": N. Yoshinari, T. Konno in *Molecular Technology, Vol. 4: Synthesis Innovation* (Eds.: H. Yamamoto, T. Kato), Wiley-VCH, Weinheim, Germany, 2019, pp. 199–230.
14 K. Nakamoto *Infrared and Raman Spectra of Inorganic and Coordination Compounds* , Wiley, New York, 1997.
15 (*a*) W.-G. Lu, J.-Z. Gu, L. Jiang, M.-Y. Tan, T.-B. Lu, *Cryst*. *Growth Des*. 2008, **8**, 192-199; (b) S.-L. Cai, S.-R. Zheng, Z.-Z. Wen, J. Fan, W.-G. Zhang, *Cryst*. *Growth Des*. 2012, **12**, 2355-2361.
16 The conductivities decreased slightly under 60% humidity (σ = 2.2 × 10^{-7} S/cm for **2** and 1.1 × 10^{-6} S/cm for **3**).
17 T. Itai, N. Yoshinari, T. Kojima, T. Konno, *Cryst*. *Growth Des*. 2017, **17**, 949-953.
18 The powder X-ray diffraction experiments indicated that the samples lost their crystallinity after the pretreatment for the ammonia adsorption experiments.
19 D. W. Kang, M. Kang, H. Kim, J. H. Choe, D. W. Kim, J. R. Park, W. R. Lee, D. Moon, C. S. Hong, *Angew*. *Chem*. *Int*. *Ed*. 2019, **58**, 16152-16155.
20 A. J. Rieth, M. Dincă, *J*. *Am*. *Chem*. *Soc*. 2018, **140**, 3461-3466.

Anion-controlled formation of hydrogen-bonded metallosupramolecular helices from a $Rh^{III}_4Zn^{II}_4$ polycarboxylate is reported.